Progress In Electromagnetics Research, PIER 82, 333–350, 2008

EXPERIMENTAL VALIDATION OF A HYBRID WIDE-ANGLE PARABOLIC EQUATION — INTEGRAL EQUATION TECHNIQUE FOR MODELING WAVE PROPAGATION IN INDOOR WIRELESS COMMUNICATIONS

G. K. Theofilogiannakos, T. V. Yioultsis, and T. D. Xenos

Department of Electrical and Computer Engineering
Aristotle University of Thessaloniki
Thessaloniki 54124, Greece

Abstract—A new full-wave Parabolic — Integral Equation Method (PE-IEM) for the simulation of wave propagation in realistic, highly complex indoor communication environments is proposed, together with an extensive validation via measurements. The method is based on a wide-angle parabolic equation, further enhanced by an integral equation correction and is capable of providing good approximations of the electromagnetic fields and the received power, incorporating all fundamental propagation mechanisms in a single simulation. For a rigorous validation, it has been applied in a complex twelve-room office space and compared with measurements at the two different frequencies of 1 GHz and 2.5 GHz. The accuracy of the approximation is within reasonably expected margins, while the method retains all the advantages of full wave methods and it also has moderate requirements of computational resources.

1. INTRODUCTION

Wireless systems and networks are considered an integral part of modern communications and their efficient planning should definitely cope with the demands of modern architecture for constructing flexible smart buildings, along with the requirement for cost reduction, network security and compliance with safety regulations. The installation of a wireless local area network (WLAN) in a highly complex environment often requires the development of a computational model, which should be able to handle the geometric complexity of the building and provide an accurate estimation of the electromagnetic power density at any location. However, the exact description of an indoor environment is

extremely difficult, since walls of bricks or concrete, doors of wood or metal, windows with single or double glazing and metallic or wooden frames have to be simulated. These completely different components are also of high contrast, regarding their electrical characteristics. In such complex settings, the occurrence of multipath effects is almost inevitable, because of multiple reflections or diffractions of the wave from the various geometric elements of the whole structure. Such effects are a source of fading, attenuation or even serious degradation of the signal integrity, due to different propagation delays for each signal path, i.e., the so-called delay spread. Therefore, analysis of the propagation characteristics in an indoor environment is necessary, especially in modern broadband applications.

Modeling of propagation in an indoor environment can be easily performed using empirical models, based on a combination of approximate calculations and interpolated measurements [1]. In general, such models may incorporate basic mechanisms of wave propagation and some kind of geometric description of the propagation channel, however in most cases they usually provide only a rough estimate of the received signal power. Therefore, more accurate and general field prediction models are frequently sought. Towards this direction, ray tracing techniques [2–17] have been extensively employed, being the state-of-the-art, especially in indoor propagation modeling. Such methods are usually based on simplified models of electromagnetic wave reflection, refraction and diffraction (such as physical optics, geometric optics or geometric theory of diffraction approximations) and, as expected, they require a large number of rays to capture the physics of the problem. Especially in highly complex practical indoor communication settings, as opposed to the more standard case of urban propagation modeling, the required number of rays may become excessive, a fact that may call for rapidly increasing computational resources for a reasonably accurate representation. On the other hand, parabolic equation approaches [18–26] have been extensively employed in problems involving propagation over a complex terrain or in urban areas. However, their applicability to indoor propagation modeling seems to be rather limited, since such techniques are more or less capable of dealing with small angles of propagation, with respect to a primary point-to-point axis.

Towards the development of a parabolic equation technique for indoor wave propagation modeling, a new full-wave model that incorporates all separate propagation mechanisms has been presented [27]. This method is based on a two-dimensional wide angle parabolic equation approach [28, 29], properly enhanced by a fast integral equation formulation, to calculate the electromagnetic field in

the interior of a building, taking into account the exact geometric form of the complex surrounding space. At a first step, a wide-angle parabolic equation method, extended with the use of a Padé approximation, is used to calculate the field into the walls, doors, windows or other obstacles, which are located in an indoor environment and are treated as penetrable objects. This is extremely convenient, since the two-dimensional problem is reduced to a successive solution of one-dimensional problems using the finite element method on the plane transverse to the paraxial direction. This calculation, however, is not appropriate to model waves that are reflected or diffracted backwards or, in general, at a high angle with respect to the main propagation axis. To overcome this problem, a proper correction of the field by a Green's function approach has been introduced, using the equivalent currents within the walls and other obstacles, computed by the PE technique. The Green's function formulation used here is based on the discrete dipole approximation, together with a point matching discretization and is merely a field correction technique that involves no matrix system solution. The hybrid method has been applied to simple models that admit analytical solutions (e.g., scattering from a dielectric cylinder) and was found to provide a significant correction to the PE approach, being able to account for backscattering or grazing waves, with moderate computational requirements. Here, a much more ambitious and realistic application is attempted, by implementing the proposed hybrid parabolic equation — integral equation method (PE-IEM) in an extremely complex office space environment and validate it with measurements. Our model is applied in a building floor of an area equal to $535\,\mathrm{m}^2$, with a total of 12 rooms. An as realistic as possible representation of the geometry of the office space has been employed, by considering walls constructed by reinforced clay masonry, clay bricks or concrete, depending on the actual construction method, wooden doors with metal frames, double glazing windows and metal frames too and all metallic structures present. To validate our model, we have performed two sets of measurements, at the signal frequencies of 1 GHz and 2.5 GHz. A thorough inspection of the simulated vs. the measured results demonstrates that the hybrid method offers a significant improvement, compared to even a wide-angle parabolic equation. The deviations between measurement and simulation is within the expected error margin, taking into account the complexity, variability and inevitably approximate description of the office space and the uncertainty involved in the measuring technique. It is noteworthy, however, that such results are obtained by a straightforward and quite simple methodology that incorporates all propagation mechanisms in a single run, without the necessity to

consider separate propagation rays.

2. THE HYBRID PARABOLIC EQUATION — INTEGRAL EQUATION METHOD

A brief description of the proposed formulation is presented here, starting from the wide angle parabolic equation scheme. In general, the parabolic equation is appropriate for solving large path propagation problems, under the assumption that the wave propagates along a main direction and at angles that do not significantly deviate from this main direction. Therefore, the electric field can be expressed in terms of a slowly varying envelope, which includes the slow variations around the propagation direction, and a phase variation along the main direction, which is assumed to be toward the x-axis,

$$\mathbf{E}(x,y,z) = \tilde{\mathbf{E}}(x,y,z)e^{jk_{ref}x}, \tag{1}$$

where $k_{ref} = k_0 n_{ref}$ is a reference propagation constant, k_0 is the free-space propagation constant and n_{ref} the reference refractive index. Using Helmholtz equation, a similar relation is obtained for the slowly varying envelope, involving both first and second order derivatives, with respect to the direction of propagation. By applying the paraxial approximation, the second order variations are considered negligible and the parabolic equation

$$\frac{\partial \tilde{\mathbf{E}}(x,y,z)}{\partial x} = j\frac{P}{2k_{ref}}\tilde{\mathbf{E}}(x,y,z), \tag{2}$$

is obtained, where the differential operator P, in two dimensions, is defined by

$$P \equiv k_0^2\left(n^2 - n_{ref}^2\right) + \frac{\partial^2}{\partial y^2}, \tag{3}$$

and variations of the field in z direction are neglected. Since in an indoor environment, excitation is usually omnidirectional and all propagation paths caused from building structures like walls, windows, obstacles etc need to be considered, it is imperative to employ a wide angle correction [28, 29], in which the second order variations of the envelope are not considered negligible. This scheme extends the use of the parabolic equation for angles up to nearly 90 degrees with respect to the primary axis. The resulting equation takes the form

$$\frac{\partial \tilde{\mathbf{E}}(x,y,z)}{\partial x} - j\frac{1}{2k_{ref}}\frac{\partial^2 \tilde{\mathbf{E}}(x,y,z)}{\partial x^2} = j\frac{P}{2k_{ref}}\tilde{\mathbf{E}}(x,y,z). \tag{4}$$

The second order derivative needs to be reformulated to involve first order derivatives only. A convenient way to do this is to write (4) in operator notation and simply solve it in terms of the first order derivative, i.e.,

$$\frac{\partial}{\partial x} = \frac{j\dfrac{P}{2k_{ref}}}{1 - j\dfrac{1}{2k_{ref}}\dfrac{\partial}{\partial x}}, \tag{5}$$

which can be thought of as a recursive relation. If (5) is applied again in order to replace the derivative in the denominator, and then substituted in (4), the compact form

$$\frac{\partial \tilde{\mathbf{E}}}{\partial x} = \frac{jN}{D}\tilde{\mathbf{E}}, \tag{6}$$

is obtained, where N and D are polynomials of the differential operator P. It is noticed that (4) can be alternatively written in the form of a forward parabolic equation

$$\frac{\partial \tilde{\mathbf{E}}}{\partial x} = j\left(\sqrt{P + k_{ref}^2} - k_{ref}\right)\tilde{\mathbf{E}}, \tag{7}$$

it becomes clear that (6) is actually a Padé approximant of order (n, d) for the exact Helmholtz operator in (7), where n and d are the highest degrees of polynomials N and D, respectively. Extensive comparisons of the wide angle scheme performance have been introduced and it is clear that a Padé approximant of order (2, 2) is sufficient, since higher order approximants do not provide a significant improvement and are computationally more demanding.

For the computational implementation of (6), discretization is performed along the x-axis, using central differences,

$$D\left(\tilde{\mathbf{E}}^{i+1} - \tilde{\mathbf{E}}^{i}\right) = j\frac{\Delta x}{2}N\left(\tilde{\mathbf{E}}^{i+1} + \tilde{\mathbf{E}}^{i}\right). \tag{8}$$

The solution on the transverse domain increases in complexity, as the order of the operator P increases. Even in the case of a $(2, 2)$ Padé approximation, the second order of P leads to a fourth order y-derivative. To solve this problem, an efficient multistep method for wide-angle beam propagation [29] can facilitate the application of the

wide-angle scheme. Equation (8) can be written in the form,

$$\tilde{\mathbf{E}}^{i+1} = \frac{\sum_{i=0}^{n} \xi_i P^i}{\sum_{i=0}^{n} \xi_i^* P^i} \tilde{\mathbf{E}}^i, \tag{9}$$

where, $\xi_0 = P^0 = 1$ and all other coefficients can be easily determined by the coefficients of the polynomials N and D [27, 29]. Hence, (9) can be cast in the factorized form

$$\tilde{\mathbf{E}}^{i+1} = \frac{(1 + a_1 P)(1 + a_2 P) \ldots (1 + a_n P)}{(1 + a_1^* P)(1 + a_2^* P) \ldots (1 + a_n^* P)} \tilde{\mathbf{E}}^i, \tag{10}$$

where the coefficients are easily found from the corresponding roots. From (10), it is obvious that a (n, n) Padé propagator may be decomposed into an n-step algorithm for which the j-th partial step takes the form

$$\tilde{\mathbf{E}}^{i+\frac{j}{n}} = \frac{(1 + a_j P)}{(1 + a_j^* P)} \tilde{\mathbf{E}}^{i+\frac{j-1}{n}}. \tag{11}$$

Each partial step involves a tridiagonal matrix system solution (block tridiagonal for the three-dimensional propagation case). Hence, the application of this technique results in a fast and unconditionally stable algorithm, with a run time which is obviously n times the run time for the conventional paraxial approximation, i.e., just twice in the case of the $(2, 2)$ Padé approximation.

To terminate the infinite space, the uniaxial anisotropic version of the perfectly matched layer (PML) has been used [30]. This dictates a modification to the field equations. For instance, the scalar wave equation in terms of the E_z component of the electric field is written in the form

$$\frac{\partial^2 \tilde{E}_z}{\partial x^2} + \frac{1}{s_y} \frac{\partial}{\partial y} \frac{1}{s_y} \frac{\partial \tilde{E}_z}{\partial y} + k_0^2 \varepsilon_r \tilde{E}_z = 0, \tag{12}$$

where s_y is the PML parameter, properly chosen to provide the necessary absorption, having also a gradual profile to reduce dispersion errors, i.e.,

$$s_y = 1 - j \tan\delta \left(\frac{y}{d}\right)^2, \quad \tan\delta = \frac{3\lambda}{4\pi d} \ln\frac{1}{R}, \tag{13}$$

where d is the PML width, y the distance from the air-PML interface and $\tan\delta$ a sufficiently large loss tangent, where R is the theoretical

desired reflection coefficient. A choice of 10^{-9} is the most appropriate for our applications.

By applying the paraxial approximation on (12), the resulting equation is

$$\frac{\partial \tilde{E}_z}{\partial x} + j\frac{1}{2k_{ref}}\frac{\partial^2 \tilde{E}_z}{\partial x^2} = -j\frac{P'}{2k_{ref}}, \tag{14}$$

where

$$P' = k_0^2\left(n^2 - n_{ref}^2\right) + \frac{1}{s_y}\frac{\partial}{\partial y}\frac{1}{s_y}\frac{\partial}{\partial y}. \tag{15}$$

Thus, (14) holds for the entire domain, if s_y is simply made equal to 1 in regions other than the PML and represents the final parabolic equation formulation which is used here. Its discretization on the transverse plane needs to be performed to calculate the field values at any plane, provided that the field on the previous plane is known.

Using the standard Galerkin procedure [31] to the wide-angle correction via the multistep technique, it is found that

$$\int \left(1 + a_j^* P'\right)\tilde{E}^{i+\frac{j}{n}}dy = \int \left(1 + a_j P'\right)\tilde{E}^{i+\frac{j-1}{n}}dy, \tag{16}$$

where by writing the revised form of the differential operator P, including PML, and standard Green's identities, the symmetric form of the Galerkin formulation is

$$\begin{aligned}&\int\left(1 + a_j^* k_0^2\left(n^2 - n_{ref}^2\right)\right)\tilde{E}'\tilde{E}^{i+\frac{j}{n}}dy - \int a_j^*\frac{1}{s_y^2}\frac{\partial \tilde{E}'}{\partial y}\frac{\partial \tilde{E}^{i+\frac{j}{n}}}{\partial y}dy\\ =&\int\left(1 + a_j k_0^2\left(n^2 - n_{ref}^2\right)\right)\tilde{E}'\tilde{E}^{i+\frac{j-1}{n}}dy - \int a_j\frac{1}{s_y^2}\frac{\partial \tilde{E}'}{\partial y}\frac{\partial \tilde{E}^{i+\frac{j-1}{n}}}{\partial y}dy\end{aligned} \tag{17}$$

and a FEM discretization results in the final system of equations

$$\begin{aligned}&\left\{\left(1 + a_j^* k_0^2\left(n^2 - n_{ref}^2\right)\right)\mathbf{T} - a_j^*\mathbf{S}\right\}\tilde{\mathbf{E}}^{i+\frac{j}{n}}\\ =&\left\{\left(1 + a_j k_0^2\left(n^2 - n_{ref}^2\right)\right)\mathbf{T} - a_j\mathbf{S}\right\}\tilde{\mathbf{E}}^{i+\frac{j-1}{n}},\end{aligned} \tag{18}$$

where

$$\mathbf{S} = \int \frac{1}{s_y^2}\frac{\partial \bar{E}'}{\partial y}\frac{\partial \bar{E}}{\partial y}dy, \quad \mathbf{T} = \int \bar{E}'\bar{E}dy \tag{19}$$

and $\tilde{\mathbf{E}}^i$ is the column vector of the wave envelope values at the nodes of the finite element mesh on the i-th transverse domain. It is obvious that (18) has to be solved n times at each step.

The presented wide-angle parabolic equation method is used to provide a fairly accurate estimation of the electric field in the interior of building structures like walls, windows, obstacles etc. It is obvious that this analysis cannot account for all propagation mechanisms, like backscattering. Hence, the idea is to consider all structures or obstacles as source volumes of secondary radiation, where the primarily computed fields within the penetrable structures act as secondary equivalent current sources. Hence, a more accurate field solution is obtained, including wave components that are reflected or diffracted from the obstacles. The corrected field can be computed from the integral equation of the first kind

$$\bar{\mathbf{E}}\left(\vec{r}\right) = \bar{\mathbf{E}}^0\left(\vec{r}\right) + \int\limits_S d^2\vec{r}\,'\bar{\bar{G}}^B\left(\vec{r},\vec{r}\,'\right) k_0^2 \Delta\varepsilon(\vec{r}\,')\bar{\mathbf{E}}^0\left(\vec{r}\,'\right), \tag{20}$$

where the integration domain includes the total surface, S, of the scatterers [32], $\bar{\bar{G}}^B(\vec{r},\vec{r\,'})$ is the free-space dyadic Green's function and $\bar{\mathbf{E}}^0\left(\vec{r}\,'\right)$ is the field approximation computed by the wide-angle parabolic equation technique. In the case of TM polarization it is

$$\bar{\bar{G}}^B\left(\vec{r},\vec{r}\,'\right) = \frac{j}{4} H_0^{(1)}\left(k_0 p\right). \tag{21}$$

Clearly, the total field at any position within free space can be easily calculated by the entire field distribution within the scatterers. Discretization of (20) is performed by the discrete dipole approximation,

$$\bar{\mathbf{E}}_i = \bar{\mathbf{E}}_i^0 + \sum_{j=1}^{N} \bar{\bar{G}}_{i,j}^B k_0^2 \Delta\varepsilon_j \bar{\mathbf{E}}_j^0 S_j, \quad i = 1, \ldots N, \tag{22}$$

where no dense matrix solution is performed, since fields are computed only outside the scatterers' domain. Recursive implementations of (20) would be also possible but are not recommended, since such an implementation would involve a dense matrix inversion and is far more demanding, in terms of computational requirements.

3. MODEL DESCRIPTION AND EXPERIMENTAL SETUP

We have chosen to model, as accurately as possible, a realistic office space consisting of twelve rooms, on the same floor, having a total area of $535\,\mathrm{m}^2$ and located at the 6th floor of Building D, School of

Engineering, Department of Electrical and Computer Engineering at the Aristotle University of Thessaloniki, Greece. The exact floor plan has been drawn in Autocad, with each separate object drawn as a polyline in a different layer, according to its material characteristics. The final drawing has been exported in .dxf format and then imported to the software, where the information about the exact dimensions, position and electrical characteristics of each structure of the whole building is retained. Plane wave excitation is assumed, since the transmitter has been placed in the exterior corridor at a sufficiently large distance away from the first object in the main direction of propagation. The two different frequencies of 1 and 2.5 GHz have been considered, representing two of the most common frequency bands for present and future mobile and wireless communication systems (GSM, UMTS and WLANs).

One of the most intricate problems involved in indoor channel simulation is the accurate representation of the electrical characteristics of the building structure components like walls, doors, windows etc. The electrical characteristics of such components, especially the conductivity, exhibit significant variations with respect to width, density, internal structure and degree of homogeneity. In a typical office building of the kind dealt with here, many different structures are involved. For example, walls between rooms may have different widths and are mainly constructed by reinforced clay blocks, with structured voids in their interior. The bricks are covered with lime-cast mortar and painted with plastic base paint. Moreover, the exterior building walls, ceilings and floors are made of reinforced concrete, with a metallic mesh of varying cell dimensions in their interior, while their exterior is covered with lime-cast incrustation and water paint. It is obvious that simulation of all those different building materials with completely different electrical characteristics is extremely difficult and in most cases unrealistic. In the literature, attempts to evaluate the equivalent electrical characteristics of most common building materials, based on measurements, have been recorded. Such results, concerning permittivity and conductivity are often contradicting and highly variable, usually due to different manufacturing and constructing techniques, a result of the different code of practice employed in each country. This is the reason why the characteristics of building materials in papers on indoor channel simulations differ substantially. For example, in the case of homogeneous brick walls the estimations of permittivity converge in values between 4 and 5.1, while values of conductivity vary from 0.0001 to 0.11 [33–35]. This is due to the large variations of the raw materials and, to the geometry of the brick web and especially to the type and materials of reinforcement. In light of such considerations, it

seems that in an indoor propagation channel all materials should be measured, a fact that is extremely difficult. Therefore, in most computational simulations of indoor propagation channels, the permittivity and conductivity of building materials are chosen in a manner that is fitted to the simulation requirements and provide the best possible representation of reality.

In this case, extensive preliminary measurements have been performed by placing a transmitting and a receiving antenna on both sides of a wall structure, since wall parameters are naturally expected to have a greater impact on the results. The equivalent permittivity and conductivity were, then, extracted from measurements and it is clearly indicated that relative permittivity values of 2.0 to 3.5 and conductivity values of 0.4 to 0.6 S/m exhibited a best fit to the measured data. The somewhat lower values of equivalent permittivity, compared to those reported in the literature are possibly due to large voids within brick walls, while the rather higher than expected equivalent conductivity values are explained by the presence of libraries, shelves and other light metallic structures outside but also within walls (pipelines, electric wires, steel reinforcements etc). For these simulations, a uniform equivalent permittivity of 2.0 and a conductivity of 0.5 S/m for the walls have been considered. Windows and wooden doors are much simpler to characterize and permittivity values of 3.0 and 2.2, respectively, have been used. Respective conductivity values have been taken equal to 0.01 and 0.0001.

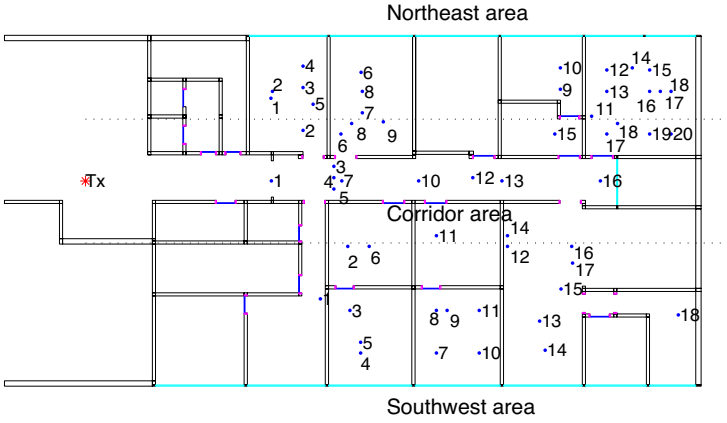

Figure 1. Floor structure split into three areas with measurement locations for the frequency of 1 GHz. The transmitter is marked as Tx and the receivers in each area are numbered.

The measurement setup included a signal generator connected to a transmitting antenna and a receiving antenna connected to a spectrum analyzer. Two basic sets of measurements have been taken, for 1 GHz and 2.5 GHz, respectively. Two signal generators have been, alternatively, used; a Marconi (model 2022D) and a Rohde & Schwarz (model SMIQ02E/03E). A diagram of the office floor under study, showing measurement locations for the frequency of

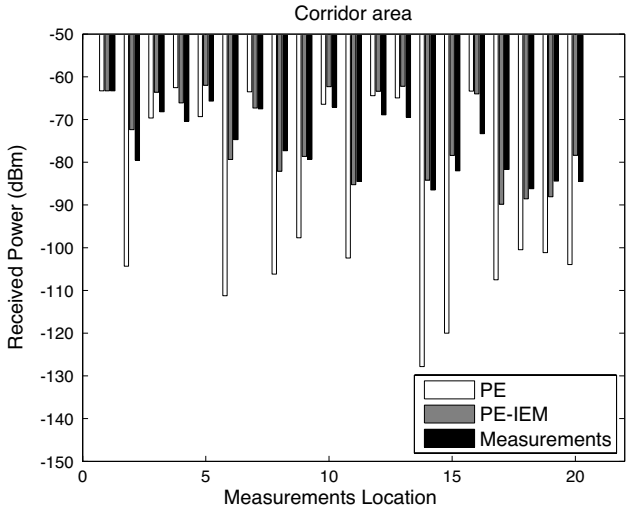

(a)

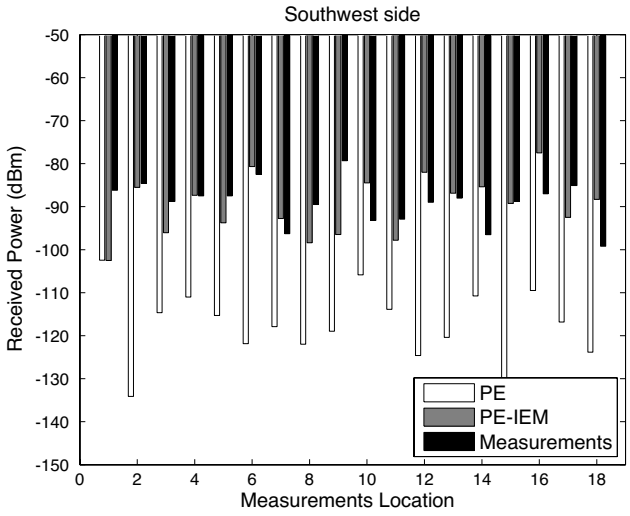

(b)

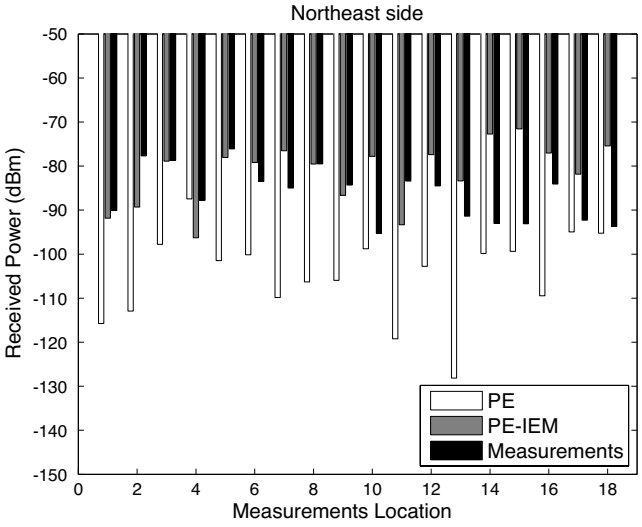

(c)

Figure 2. Comparison of PE-IEM and PE with measurements for the frequency of 1 GHz in (a) Corridor, (b) Southwest and (c) Northeast area.

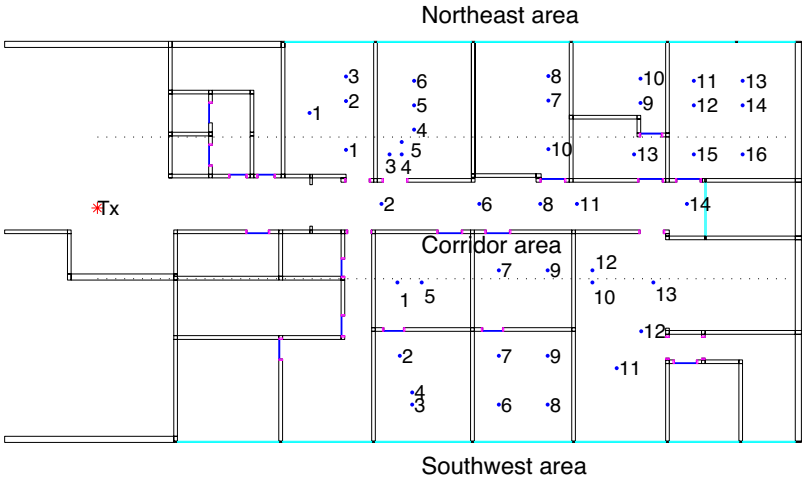

Figure 3. Floor structure split into three areas with measurement locations for the frequency of 2.5 GHz. The transmitter is marked as Tx and the receivers in each area are numbered.

1 GHz is given in Fig. 1. The transmitting wideband discone antenna (Electro-metrics EM 6105) was placed at a point in the external corridor and the receiving omni-directional antenna (Electro-metrics EM 6865) was placed, successively, at each one of the measurement locations. The input power was set to 0 dBm, while the received power was recorded by an Anritsu Spectrum Analyzer (Spectrum Master MS2721B). Measurements have been taken inside all accessible rooms and the corridor, in a total of 56 and 43 locations for the first and second set of measurements, respectively.

4. COMPARISON OF COMPUTATIONAL AND EXPERIMENTAL RESULTS — DISCUSSION

It has been decided to split the office space into three areas, the northeast, the southwest and the corridor area, as it is shown in Fig. 1, for the sake of better measurement classification. The transmitter location is marked by Tx and the receiver locations in each building room are assigned a separate number. Comparisons of the proposed hybrid wide-angle PE-IEM method with the wide-angle PE method without correction and measurements in the corridor, southwest and northwest areas are presented in Figs. 2(a), (b) and (c), respectively, for the frequency of 1.0 GHz. Similarly, transmitter and measurement locations for the frequency of 2.5 GHz are shown in Fig. 3, while comparative results for the corridor, southwest and northwest

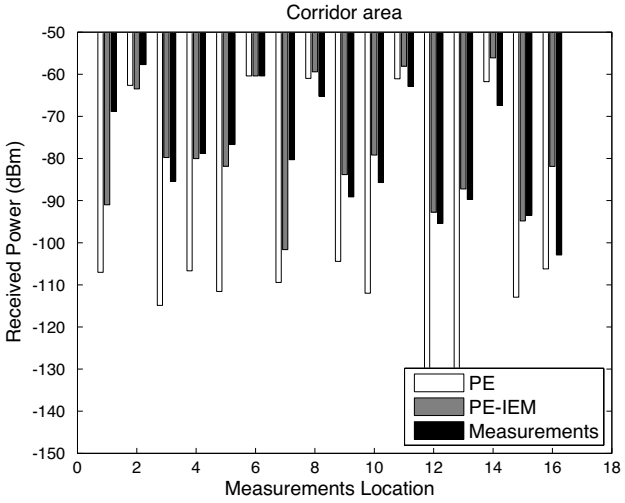

(a)

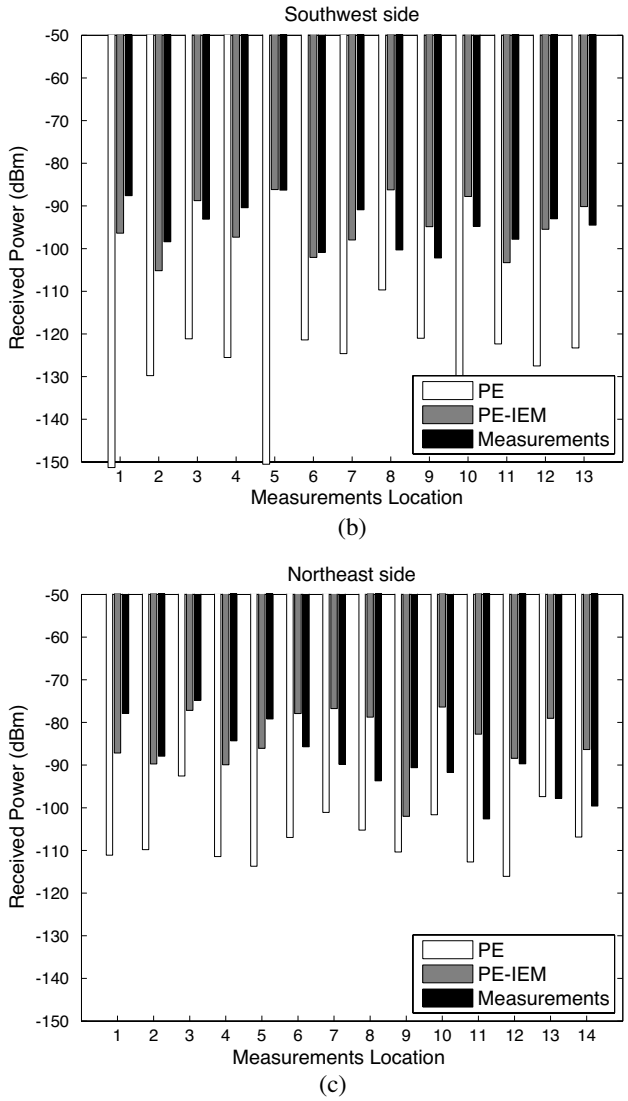

Figure 4. Comparison of PE-IEM and PE with measurements for the frequency of 2.5 GHz: (a) Corridor, (b) Southwest and (c) Northeast area.

areas are given in Figs. 4(a), (b) and (c), respectively. Results in Figs. 2 and 4 indicate that the introduction and implementation of the integral equation formulation provides a clear enhancement

of accuracy, compared to the wide-angle parabolic equation alone. Generally, the accuracy of the hybrid technique increases at locations close to the corridor. Higher deviations are recorded for positions far from the symmetry axis, since the received power may be due to a multitude of separate propagating, refracted, reflected and diffracted waves. Nevertheless, the results are definitely within the expected error margins and can be considered acceptable, from an engineering point of view. It is emphasized that the geometric configuration and material characteristics in a building environment is so complex, with several features that cannot be accurately determined or modeled and this fact is naturally expected to compromise the accuracy of the computational technique, as opposed to comparisons with simple analytical solutions. For the same reason, it is difficult to determine whether some larger errors, reported for the most remote room of the northwest area are due to poor modeling of the surrounding space or is an indication of possible limitations of the computational method.

5. CONCLUSIONS

In this paper, a hybrid parabolic equation — integral equation formulation has been successfully applied in a realistic highly complex indoor environment and validated with measurements. In general, the proposed technique has been shown to provide fairly accurate estimates of the received power density at any location of a complex indoor environment and has the potential to become a serious alternative to ray tracing techniques, which are the primary methods of choice in modern mobile and wireless communications planning.

REFERENCES

1. Bertoni, H. L., *Radio Propagation for Modern Wireless Systems*, Prentice Hall, New Jersey, 2000.
2. Honcharenko, W., H. L. Bertoni, and J. Dailing, "Mechanism governing propagation on single floors in modern office buildings," *IEEE Trans. Antennas and Propagation*, Vol. 41, No. 4, 496–504, 1992.
3. Chen, S. H. and S. K. Jeng, "An SBR/image approach for radio wave propagation in indoor environments with metallic furniture," *IEEE Trans. Antennas Propagation*, Vol. 45, No. 1, 98–106, 1997.
4. Ghobadi, G., P. R. Shepherd, and S. R. Pennock, "2D ray-tracing model for indoor radio propagation at millimeter frequencies and

the study of diversity techniques," *IEE Proc. - Microw. Antennas Propagation*, Vol. 145, No. 4, 349–353, 1998.

5. Yang, C.-F., B.-C. Wu, and C.-J. Ko, "A ray-tracing method for modeling indoor wave propagation and penetration," *IEEE Trans. Antennas Propagation*, Vol. 46, No. 6, 907–919, 1998.
6. Ji, Z., B.-H. Li, H.-X. Wang, H.-Y. Chen, and Y.-G. Zhou, "An improved ray-tracing propagation model for predicting path loss on single floors," *Microw. and Optical Tech. Letters*, Vol. 22, No. 1, 39–41, 1999.
7. Agelet, F. A., et al., "Efficient ray-tracing acceleration techniques for radio propagation modeling," *IEEE Trans. on Vehicular Technology*, Vol. 49, No. 6, 2089–2104, 2000.
8. Wang, Y., S. Safavi-Naeini, and S. K. Chaudhuri, "A hybrid technique based on combining ray tracing and FDTD methods for site-specific modeling of indoor radio wave propagation," *IEEE Trans. Antennas Propagation*, Vol. 48, No. 5, 743–754, 2000.
9. Athanasiadou, G. E. and A. R. Nix, "A novel 3-D indoor ray-tracing propagation model: The path generator and evaluation of narrow-band and wide-band predictions," *IEEE Trans. Vehicular. Technology*, Vol. 49, No. 4, 1152–1168, 2000.
10. Remley, K. A., H. R. Anderson, and A. Weisshaar, "Improving the accuracy of ray-tracing techniques for indoor propagation modeling," *IEEE Trans. Vehicular Technology*, Vol. 49, No. 6, 2350–2358, 2000.
11. De Adana, F. S., O. G. Blanco, I. G. Diego, J. P. Arriaga, and M. F. Catedra, "Propagation model based on ray tracing for the design of personal communication systems in indoor environments," *IEEE Trans. Vehicular Technology*, Vol. 49, No. 6, 2105–2112, 2000.
12. Attiya, A. M. and E. El-Diwany, "A time domain incremental theory of diffraction: scattering of electromagnetic pulsed plane waves," *J. of Electromagn. Waves and Appl.*, Vol. 18, No. 2, 205–207, 2004.
13. Teh, C. H., F. Kung, and H. T. Chuah, "A path-corrected wall model for ray-tracing propagation modeling," *J. of Electromagn. Waves and Appl.*, Vol. 20, No. 2, 207–214, 2006.
14. Jin, K.-S., "Fast ray tracing sing a space-division algorithm for RCS prediction," *J. of Electromagn. Waves and Appl.*, Vol. 20, No. 1, 119–126, 2006.
15. Wang, S., H. B. Lim, and E. P. Li, "An efficient ray-tracing method for analysis and design of electromagnetic shielded room

systems," *J. of Electromagn. Waves and Appl.*, Vol. 19, No. 15, 2059–2071, 2005.

16. Chen, C. H., C.-L. Liu, C.-C. Chiu, and T.-M. Hu, "Ultra-wide band channel calculation by SBR/image techniques for indoor communication," *J. of Electromagn. Waves and Appl.*, Vol. 20, No. 1, 41–51, 2006.
17. Teh, C. H. and H. T. Chuah, "An improved image-based propagation model for indoor and outdoor communication channels," *J. of Electromagn. Waves and Appl.*, Vol. 17, No. 1, 31–50, 2003.
18. Zaporozhets, A. A. and M. F. Levy, "Modeling of radiowave propagation in urban environment with parabolic equation method," *Electron. Lett.*, Vol. 32, No. 17, 1615–1616, 1996.
19. Donohue, D. J. and J. R. Kuttler, "Propagation modeling over terrain using the parabolic wave equation," *IEEE Trans. Antennas Propagation*, Vol. 48, 260–277, 2000.
20. Zelley, C. A. and C. C. Constantinou, "A three-dimensional parabolic equation applied to VHF/UHF propagation over irregular terrain," *IEEE Trans. Antennas Propagation*, Vol. 47, 1586–1596, 1999.
21. Sevgi, L., F. Akleman, and L. B. Felsen, "Groundwave propagation modeling: Problem-matched analytic formulations and direct numerical techniques," *IEEE Antennas Propagation Mag.*, Vol. 44, No. 1, 55–75, 2002.
22. Janaswamy, R., "Path loss predictions in the presence of buildings on flat terrain: A 3-D vector parabolic equation approach," *IEEE Trans. Antennas Propagation*, Vol. 51, No. 8, 1716–1728, 2003.
23. Awadallah, R. S., J. Z. Gehman, J. R. Kuttler, and M. H. Newkirk, "Effects of lateral terrain variations on tropospheric radar propagation," *IEEE Trans. Antennas Propagation*, Vol. 53, No. 1, 420–434, 2005.
24. Oraizi, H. and N. Noori, "Least square solution of the 3-D vector parabolic equation," *J. of Electromagn. Waves and Appl.*, Vol. 20, No. 9, 1175–1187, 2006.
25. Noori, N. and H. Oraizi, "Evaluation of MIMO channel capacity in indoor environments using vector parabolic equation method," *Progress In Electromagnetics Research B*, Vol. 4, 13–25, 2008.
26. Graglia, R. D., "The parabolic equation method for the high-frequency scattering from a convex perfectly conducting wedge with curved faces," *J. of Electromagn. Waves and Appl.*, Vol. 21, No. 5, 585–598, 2007.

27. Theofilogiannakos, G. K., T. V. Yioultsis, and T. D. Xenos, "An efficient hybrid parabolic equation — Integral equation method for the analysis of wave propagation in highly complex indoor communication environments," *Wireless Personal Communications, Springer*, Vol. 43, No. 2, 495–510, 2007.
28. Hadley, G. R., "Wide-angle beam propagation using Padé approximant operators," *Optics Letters*, Vol. 17, No. 20, 1426–1428, 1992.
29. Hadley, G. R., "Multistep method for wide-angle beam propagation," *Optics Letters*, Vol. 17, No. 24, 1743–1745, 1992.
30. Sacks, Z. S., D. M. Kingsland, R. Lee, and J.-F. Lee, "A perfectly matched anisotropic absorber for use as an absorbing boundary condition," *IEEE Trans. Antennas Propagation*, Vol. 43, No. 12, 1460–1463, 1995.
31. Jin, J., *The Finite Element Method in Electromagnetics*, Wiley, New York, 1993, 2002.
32. Collin, R. E., *Field Theory of Guided Waves*, IEEE Press, New York, 1990.
33. Hu, C. F., J. D. Xu, N. J. Li, and L. X. Zhang, "Indoor accurate RCS measurements techniques on UHF band," *Progress In Electromagnetics Research*, PIER 81, 279–289, 2008.
34. Amirhosseini, M. K., "Three types of walls for shielding enclosures," *J. of Electromagn. Waves and Appl.*, Vol. 19, No. 6, 827–838, 2005.
35. Safaai-Jazi, A., S. M. Riad, A. Muqaibel, and A. Bayram, "Ultra-wideband propagation measurements and channel modeling; through-the-wall propagation and material characterization," *DARPA NETEX Program*, 2002.